Surface Science 687 (2019) 1–6

Contents lists available at ScienceDirect

Surface Science

journal homepage: www.elsevier.com/locate/susc

Formation of magic gold fingers under mild and relevant experimental conditions

Jesse A. Phillips, K.P. Boyd, I. Baljak, L.K. Harville, Erin V. Iski*

Department of Chemistry and Biochemistry, The University of Tulsa, Keplinger Hall, 800 S. Tucker Dr., Tulsa, OK 74104, United States

ARTICLE INFO

Keywords:
Magic gold fingers
EC-STM
Amino acids
Relevant experimental conditions
Mild electric fields

ABSTRACT

Using electrochemical scanning tunneling microscopy (EC-STM) at room temperature and under a liquid layer, magic gold fingers were grown in the presence of three different amino acids, N-Boc-L-Isoleucine, L-Tyrosine, and L-Phenylalanine. The surface was modified using a very mild electric field induced by the tip and the interaction of amino acid molecules with the Au(111) surface. When 0.28 V vs Ag/AgCl was supplied to the working electrode, an extremely small tunneling current of 0.07 nA and a bias of −0.1 V could be used to induce the surface modification. It is clear that a combination of the interaction of the molecules with the surface and the external potential led to the formation of the fingers. The results demonstrate the first instance of this surface structure formed at such mild electric field conditions *and* imaged under relevant experimental parameters, i.e. at room temperature and in a fluid cell.

1. Introduction

In its current state, the industry centered around the manufacturing and commercialization of electronics has shown a propensity for the constant reduction of proportions leading to increased interest in the fields of surface science and nanoarchitecture [1,2]. In order to successfully and accurately form these structures at such an incredibly minuscule domain, it has been demonstrated that it is vital to maintain both atomic and molecular control of the surface of the substrate [3,4]. Of the various forms of surface metrology that have arisen over the past two decades, few give more control over such manipulation as scanning probe microscopy, or more specifically, scanning tunneling microscopy (STM) [5–10]. The majority of these studies focus on the use of single crystals due to the atomically flat nature of the crystal surface, as well as known defect sites that manifest as step edges, adatoms, or, in the case of Au(111), the herringbone reconstruction [11–13]. These metallic surfaces, when exposed to various adsorbates, such as amino acids, regularly demonstrate the formation of new topographical features [3,14–16]. These new surface species can take on many forms based on the experimental conditions and have a strong dependence on external factors such as temperature gradients as well as electrochemical manipulation [17–22]. One such surface structure that has garnered much attention recently is that of the nanowire, a low dimensional structure that can form on a Au(111) surface, and was reported by Guo et al. in great detail [23,24]. In that work, the formation of “magic gold fingers” was directly facilitated by a high electric field near the surface using the STM tip. This high electric field seemingly promoted Au surface atoms, specifically those near step edges, to “break away” from the surface and immediately re-adsorb near the step edge to form nucleation sites for further deposition and the subsequent formation of Au nanowires [25].

An important factor of the results demonstrated by Guo et al. and the Totó research group was the necessity of an extremely high electric field in order to induce the formation of these nanowires on the Au (111) surface [23–25]. The use of such extreme conditions, relative to the scale of experimentation, leaves little room for additional work on the surface. However, it has been shown that by modifying the surface prior to scanning, the formation can be induced at milder experimental conditions [3,26–29]. Additionally, amino acids are known to interact and modify surfaces and have been the subject of many recent experiments [30–33], some focusing on their uses in molecular electronics [34,35] and biosensors [36,37]. Importantly, amino acids have also been shown to induce the formation of nanowires/gold fingers [26,27]. The aim of this report is to elaborate on the successful formation under mild conditions of these magic gold fingers formed on a Au(111) surface, which has been treated with amino acids and imaged under relevant conditions using electrochemical scanning tunneling microscopy (EC-STM).

* Corresponding author.
E-mail addresses: jesse-phillips@utulsa.edu (J.A. Phillips), kpb878@utulsa.edu (K.P. Boyd), irb656@utulsa.edu (I. Baljak), Lkh106@utulsa.edu (L.K. Harville), erin.iski@utulsa.edu (E.V. Iski).

https://doi.org/10.1016/j.susc.2019.04.005
Received 28 February 2019; Accepted 24 April 2019
Available online 25 April 2019

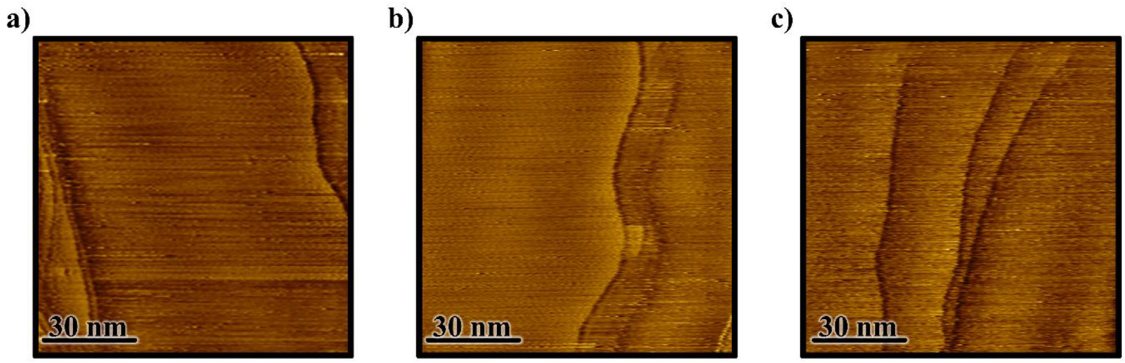

Fig. 1. a) EC-STM image of the clean, bare Au(111) surface before addition of N-Boc-L-Isoleucine. V_{sample} = 0.70 V, I_t = 0.17 nA, Bias = −0.30 V. b) EC-STM image of the clean, bare Au(111) surface before addition of L-Tyrosine. V_{sample} = 0.70 V, I_t = 0.17 nA, Bias = −0.30 V. c) EC-STM image of the clean, bare Au(111) surface before addition of L-Phenylalanine. V_{sample} = 0.70 V, I_t = 0.17 nA, Bias = −0.30 V.

2. Materials and methods

All of the experiments were performed using *in-situ* scanning tunneling microscopy (STM) under ambient conditions on an Agilent/Keysight PicoScan 5500 scanning probe microscope. The Agilent/Keysight PicoScan 5500 is capable of performing EC-STM in real time with an internal biopotentiostat and a three-electrode set-up. For the three-electrode system, the Au(111) crystal (Princeton Scientific Corp.) acted as the working electrode while a $Pt_{0.8}Ir_{0.2}$ wire (Nanoscience Instruments) was used as a counter electrode to facilitate electron flow, and a Pt wire (Alfa Aesar, ≥99.997%) was used as a reference electrode. The Pt wire is understood to be a quasi-reference electrode and was referenced against a known Ag/AgCl electrode in saturated KCl to obtain an open circuit potential of +0.63 V vs. Ag/AgCl [38]. All potentials in this manuscript are therefore reported vs. Ag/AgCl. The tips used in all of the experiments were Apiezon wax coated, $Pt_{0.8}Ir_{0.2}$ wire tips (Keysight Technologies) designed to allow less than 70 pA of leakage current into the system. Furthermore, in order to perform *in-situ* measurements of the surface, a fluid cell was used to house the electrodes, the electrolyte solution, and the surface (working electrode). Due to the extreme chemical sensitivity inherit to both *in-situ* and EC-STM, all components of the fluid cell, as well as the crystal itself, must be subjected to a rigorous cleaning procedure. This procedure included the daily soaking of all materials in freshly prepared piranha solution (1:3 H_2O_2 (30%):H_2SO_4) to ensure any contaminating organics were removed.

For this study, the surface and working electrode was a Au single crystal cut along the (111) plane with an orientation accuracy of < 0.1° and polished to a surface roughness < 0.01 µm. Sample preparation included annealing the crystal under a 1,000 K hydrogen flame for 10 min to ensure that the surface was clean and flat. Once finished, the fluid cell was constructed and a 0.1 M $HClO_4$ solution was added as the electrolyte. This electrolyte was used due to its well-known interactions with the gold surface [18,19,39–48]. Several amino acids were investigated for this study, all of which were of the L stereoisomer and of 98+% purity. N-Boc-L-Isoleucine was purchased from Alfa Aesar, L-tyrosine from Sigma-Aldrich, and L-Phenylalanine from VWR.

3. Results and discussion

This report discusses the observation of magic gold fingers for the first time at mild scanning conditions *and* at room temperature under a liquid layer. The disruption of the surface morphology was observed after the deposition of amino acids on a Au(111) surface and while performing EC-STM to apply a constant surface potential to the system. The EC-STM uses a 3-electrode fluid cell which allows the electrochemical manipulation of the surface in real time. With the fluid cell in place, the crystal was held at a positive potential for two hours as a means to electrochemically remove the $22\,x\,\sqrt{3}$, or herringbone, surface reconstruction innate to bare Au(111). The flattening of the gold surface is a well-documented phenomenon and allows for the study of surface adsorption devoid of a templating reconstruction [18,19,46,47,49]. With the reconstruction gone, the surface was imaged to ensure that the crystal was flat and without contamination. Cyclic voltammograms (CVs) were also used to indicate the cleanliness of the Au surface (Figure S1) as the clean Au(111) surface has a well-defined electrochemical signature [46–48,50]. Fig. 1 shows the crystal surface before the addition of a) N-Boc-L-Isoleucine, b) L-Tyrosine, and c) L-Phenylalanine. In all three instances, it can be observed that the gold surface is without any major surface structures such as islands or etch pits, which would indicate an improper surface for investigation. It is also clear that the herringbone reconstruction is not present. Additionally, the surface flatness of each system was shown to be in the pm domain, again indicating the cleanliness of the surface (Fig. S2, Table S1).

Once confirmation of a contaminant and defect free surface was obtained, an amino acid (AA) solution of interest was introduced to the fluid cell. Each amino acid solution was 0.5 mM AA in 0.1 M $HClO_4$. The reasoning behind the use of an acidic electrolyte is beyond the scope of this letter, but will be discussed in greater detail in a future full-length research article. Generally, this electrolyte is often used in the EC-STM literature and has a well characterized solvent window for the reference electrode [47,51]. Once added to the cell, amino acid adsorption to the surface was promoted through the application of an external potential across the surface, 0.28 V vs Ag/AgCl [52–57]. To ensure deposition had occurred, scanning took place at a greater potential than the potential necessary to promote adsorption, which is known as an overpotential. While scanning at an overpotential for N-Boc-L-Isoleucine, it was found that rather than developing the surface species originally under investigation, gold fingers began to manifest instead. The application potential for each amino acid was determined through the use of cyclic voltammetry performed at the surface (Figure S3), however, a constant overpotential of ~0.28 V was consistently used due to its experimentally determined ability to assist in the formation of gold fingers. The effect of scanning at the active adsorption potential as measured in the AA CVs will be reported in a future publication. Potentials are typically used in EC-STM measurements as a means to pull or hold molecules on the surface, which would otherwise be moving extremely fast at room temperature [58–63]. Once the potential was applied, the surface was imaged in order to observe any surface modification induced by the potential and the adsorption of the amino acids. The results of these images are shown in Fig. 2a–c, which represent the growth of magic gold fingers in N-Boc-L-Isoleucine (2a), L-Tyrosine (2b), and L-Phenylalanine (2c) solutions, respectively. The Palmer group first noticed the formation of these types of structures while scanning the surface under an extremely high electric field [23,24].

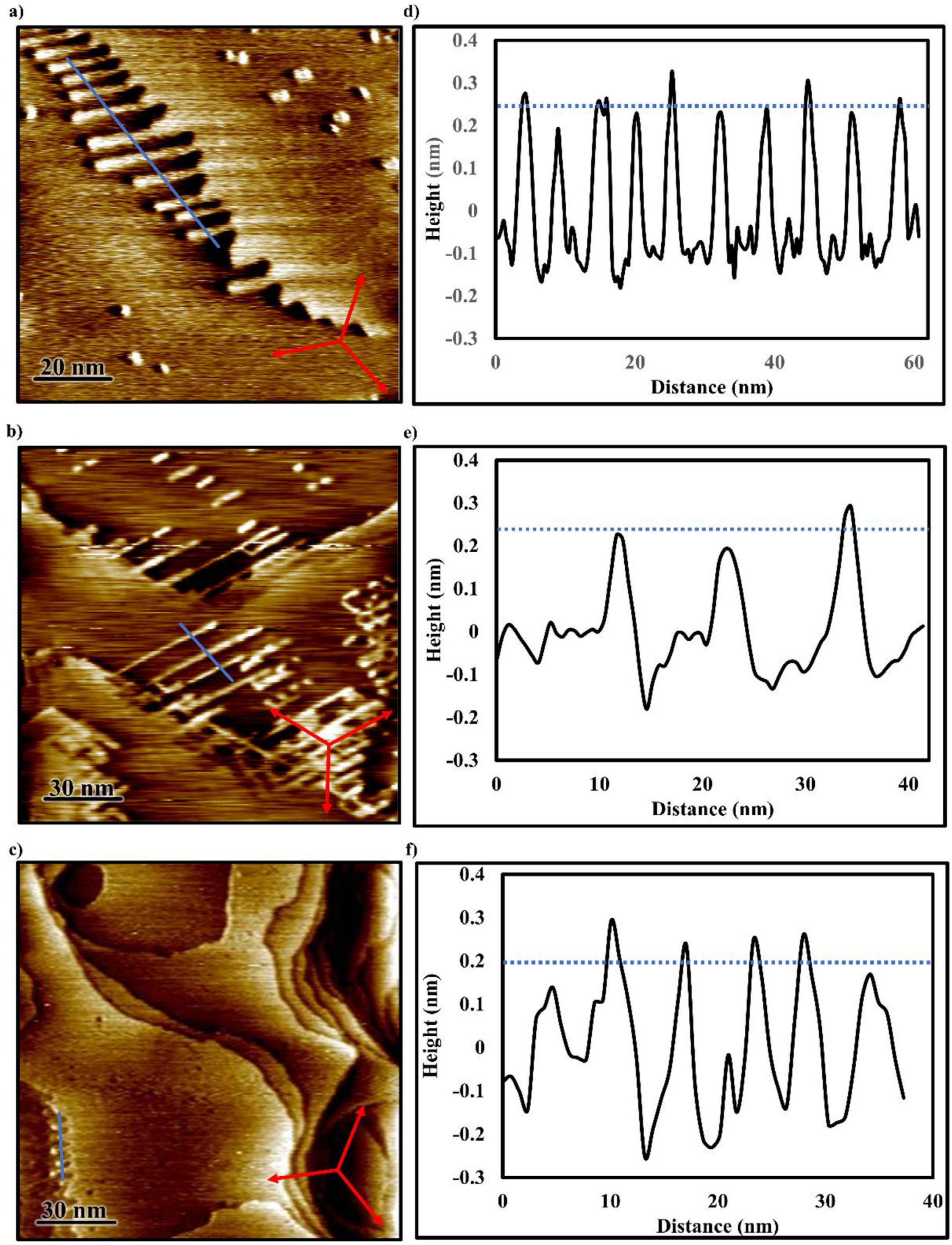

Fig. 2. a) EC-STM image of the Au(111) surface after addition of 0.55 mM N-Boc-L-Isoleucine. While scanning at $V_{sample} = 0.28$ V, $I_t = 0.07$ nA, Bias = −0.1 V, gold nanofingers began to form along the direction of the close-packed orientation of the crystal (red inset). b) EC-STM image of the Au(111) surface after addition of 0.55 mM L-Tyrosine. While scanning at $V_{sample} = 0.28$ V, $I_t = 0.07$ nA, Bias = −0.1 V, gold nanofingers began to form. c) EC-STM image of the Au(111) surface after addition of 0.55 mM L-Phenylalanine. While scanning at $V_{sample} = 0.33$ V, $I_t = 0.07$ nA, Bias = 0.2 V, gold nanofingers began to form. d) Height profile of Au fingers after deposition of N-Boc-L-Isoleucine. Average height = 0.24 ± 0.05 nm. e) Height profile of Au fingers after deposition of L-Tyrosine. Average height = 0.22 ± 0.05 nm. f) Height profile of Au fingers after deposition of L-Phenylalanine. Average height = 0.20 ± 0.06 nm. A blue dotted line shows the average height of each profile, which is 0.24 nm, corresponding to the known height of a Au step.

This field was caused by increasing the tunneling current of the STM to 30 nA, over 400 times larger than the tunneling current used to obtain the images in Fig. 2a–c. The directionality of the fingers was determined to coincide with the close-packed direction of the underlying surface within a 60° rotation of the <110> faceted step edge. The inset of Fig. 2a–c shows the directionality of the fingers grown on our crystal, which are in agreement with the directions reported by Guo et al. [23,24]. Importantly, the directionality of the inset changes from image to image because the crystal's orientation changes daily, but it can always be determined from the step edge directions. Figs. 2d–f show the

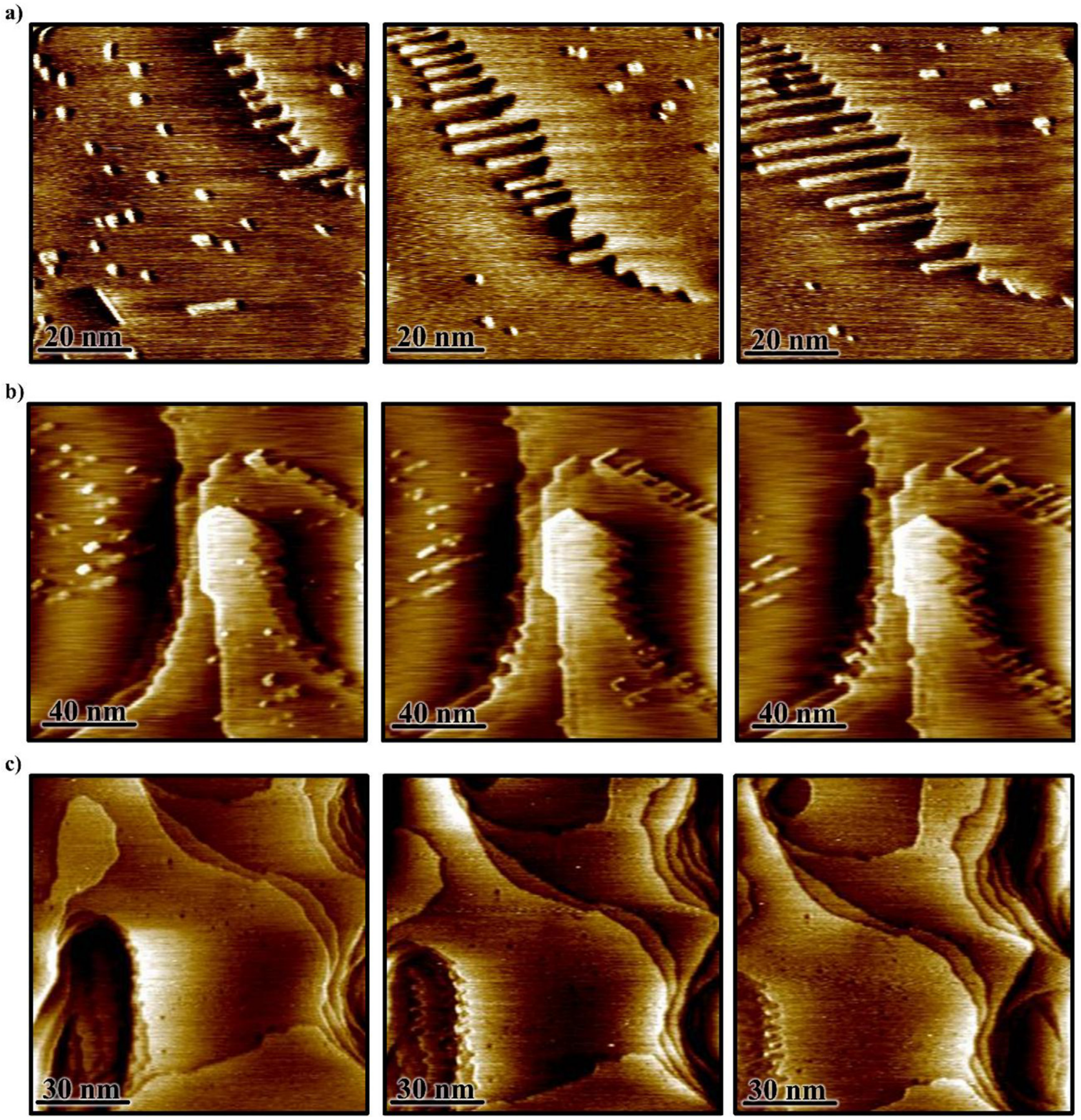

Fig. 3. a) Time-lapsed EC-STM images of N-Boc-L-Isoleucine over ~10 min. Images show the amino acid assisted growth of nanofingers on Au(111) as the tip rasters across the surface. V_{sample} = 0.28 V, I_t = 0.07 nA, Bias = −0.1 V. b) Time-lapsed EC-STM images of L-Tyrosine over ~10 min. Images show the amino acid assisted growth of nanofingers on Au(111) as the tip rasters across the surface. V_{sample} = 0.28 V, I_t = 0.07 nA, Bias = −0.1 V. c) Time-lapsed EC-STM images of L-Phenylalanine over ~10 min. Images show the amino acid assisted growth of nanofingers on Au(111) as the tip rasters across the surface. V_{sample} = 0.33 V, I_t = 0.07 nA, Bias = 0.2 V.

height profiles of the nanofingers across the surface. The average value of the heights is 0.24 ± 0.06 nm, which is in good agreement with previously reported values and the height of a Au step [23,24,28].

As mentioned, the formation of these gold nanofingers was achieved at a much lower tunneling current, which is also similar to results obtained by other groups [27,28]. However, the results detailed herein differ in key aspects. In the case of the work by Arima et al., they determined that porphyrins anchored to the surface via thiol groups could assist in the movement of gold cluster assemblies on the surface under the effect of the electric field induced by the tip [28]. The tip-induced electric field was obtained with the tunneling current at approximately 1 nA, which was much lower than what was previously reported [11,23–25]. However, this is still nearly 15 times larger than the current used in this study, i.e. 0.07 nA. Furthermore, the reaction of thiols with the gold surface varies considerably from that of amino acids absent of a sulfur group as it is well-known that sulfur covalently binds to the Au and removes Au atoms from the surface [64–68]. The amino acid, Lysine, was used in the study by Wilson et al. which is more similar to our work as that molecule lacks a sulfur group, like all of the ones included here. In that work, the formation of the gold nanofingers was observed along the close-packed direction of the Au surface, and they were obtained at lower tunneling currents, 0.2–1 nA [27], a value still twice as large as those used to obtain the images in Fig. 2a–c at their lowest and 15 times larger at the highest. Finally, all of the studies mentioned above were performed using Ultra-High Vacuum STM (UHV-STM), which maintains a pristine environment devoid of contamination and often considered quite far from “real-world” conditions [69–71].

Although there are some characteristic differences between the experimental parameters reported in past literature and those reported here, the key variance lies in the unique capabilities of EC-STM. The magnitude of the tunneling current is always considerably less than those presented in other types of STM studies, yet conditions within the EC environment still allow for the observation of the magic gold fingers. The ability to hold an external potential across the surface, independent of the tunneling bias, is in part what allows this to occur. The effect of the external potential was demonstrated when the potential was removed and nanofingers were not observed (Fig. S4). Once the potential was reactivated, the nanofingers began to grow once again. Importantly, on a molecular-level, the applied external potential was driving an interaction of the amino acid molecules with the surface while also altering the energetic landscape of the Au surface itself. This molecular interaction was leading to the disruption and movement of the Au surface atoms [72–77]. The applied potential and the presence of the amino acids went hand-in-hand in promoting the appearance and growth of the magic gold fingers.

Additionally, due to the nature of *in-situ* STM, it was possible to gather the images in liquid and at room temperature allowing for the observation of the fingers in more relevant environmental conditions. This is the first observation of the magic fingers in an environment outside of UHV, which is critical to the application of these findings to systems closer to the “real-world”. Fig. 3 shows the real-time growth of the fingers in the case of all three amino acids. Each panel from left to right of Fig. 3a–c is a consecutive frame taken roughly 3 min apart while rastering across the surface. Furthermore, all of the other reports have been performed under UHV with the amino acids already dosed onto the surface. This is the first example of the dynamic adsorption of the amino acids and their effect on the growth of the fingers. Through the use of EC-STM while performing *in-situ* imaging, not only was the formation of magic gold fingers successfully observed, but it was accomplished in real time with precise control of the interaction of the amino acid molecules with the surface. This process allowed the phenomenon to occur at extremely mild conditions and outside of UHV.

4. Conclusion

The ability to manipulate surfaces electrochemically while imaging in real time is a process that is unique to the EC-STM instrument. Furthermore, it allows all of the imaging to take place under ambient conditions and in liquid, which is a distinctive set of conditions for the observation of magic gold fingers. The growth of these gold nanofingers was studied with EC-STM after the adsorption of three amino acids, N-Boc-L-Isoleucine, L-Tyrosine, L-Phenylalanine. As seen previously, the fingers grew along the <110> close-packed direction at roughly a 60° rotation from the step-edge nucleation site, and they maintained a characteristic height of ~0.25 nm, the height of a single Au atomic step. The magic gold fingers were formed due to the combination of an applied external potential, which alters the amount of energy it takes to restructure the surface and governs molecular interactions of molecules at the surface, and the deposition of amino acids, which are known to assist in moving atoms on metal surfaces. These structures have been of great interest and study over the past decade and now can be obtained much more readily at mild conditions, as well as imaged and modified in closer to “real-world” conditions. With this advance, the opportunity to study and use these gold nanowires in applications beyond fundamental studies becomes more approachable.

Declaration

The authors declare no competing financial interests.

Acknowledgments

The authors gratefully acknowledge the financial support from The University of Tulsa. Additional support for this work was provided by the National Science Foundation under award OIA-1833019. Author J.A.P. was supported in part through the Graduate Research Grant Program through the Office of Research and Sponsored Programs at The University of Tulsa. Authors L.K.H., K.P.B., and I.B. were supported through both the Chemistry Summer Undergraduate Research Program and the Tulsa Undergraduate Research Challenge offered through The University of Tulsa.

Supplementary materials

Supplementary material associated with this article can be found, in the online version, at doi:10.1016/j.susc.2019.04.005.

References

[1] R.W. Hart, H.S. White, B. Dunn, D.R. Rolison, 3-D microbatteries, Electrochem. Commun. 5 (2003) 120–123.
[2] J.W. Long, B. Dunn, D.R. Rolison, H.S. White, Three-dimensional battery architectures, Chem. Rev. 104 (2004) 4463–4492.
[3] J.A. Boscoboinik, R.R. Kohlmeyer, J. Chen, W.T. Tysoe, Efficient transport of gold atoms with a scanning tunneling microscopy tip and a linker molecule, Langmuir 27 (2011) 9337–9344.
[4] R. Otero, F. Rosei, F. Besenbacher, Scanning tunneling microscopy manipulation of complex organic molecules on solid surfaces, Annu. Rev. Phys. Chem. 57 (2006) 497–525.
[5] S.-W. Hla, Scanning tunneling microscopy single atom/molecule manipulation and its application to nanoscience and technology, J. Vac. Sci. Technol. B 23 (2005) 1351–1360.
[6] L. Bartels, G. Meyer, K.-H. Rieder, Controlled vertical manipulation of single CO molecules with the scanning tunneling microscope: a route to chemical contrast, Appl. Phys. Lett. 71 (1997) 213–215.
[7] L. Bartels, G. Meyer, K.H. Rieder, Basic steps of lateral manipulation of single atoms and diatomic clusters with a scanning tunneling microscope tip, Phys. Rev. Lett. 79 (1997) 697–700.
[8] J.A. Stroscio, D.M. Eigler, Atomic and molecular manipulation with the scanning tunneling microscope, Science 254 (1991) 1319–1326.
[9] L.J. Whitman, J.A. Stroscio, R.A. Dragoset, R.J. Celotta, Manipulation of adsorbed atoms and creation of new structures on room-temperature surfaces with a scanning tunneling microscope, Science 251 (1991) 1206–1210.
[10] D.M. Eigler, E.K. Schweizer, Positioning single atoms with a scanning tunnelling microscope, Nature 344 (1990) 524.
[11] F. Yin, R.E. Palmer, Q. Guo, Critical stability of gold nanofingers on a zero-gradient stepped surface, J. Phys. 21 (2009) 445001.
[12] H.-C. Jeong, E.D. Williams, Steps on surfaces: experiment and theory, Surf. Sci. Rep. 34 (1999) 171–294.
[13] M. Giesen, Step and island dynamics at solid/vacuum and solid/liquid interfaces, Prog. Surf. Sci. 68 (2001) 1–154.
[14] A. González-Carrazco, J. Valenzuela-Benavides, Scanning tunneling microscopy study of the relaxation mechanism of a Au(100) nanostructure, J. Nanosci. Nanotechnol. 8 (2008) 6603–6607.
[15] P.A. Thiel, M. Shen, D.-J. Liu, J.W. Evans, Coarsening of two-dimensional nanoclusters on metal surfaces, J. Phys. Chem. C 113 (2009) 5047–5067.
[16] K. Morgenstern, E. Lægsgaard, F. Besenbacher, STM study of step dynamics around a bulk dislocation intersection with a Ag(111) surface, Phys. Rev. B 71 (2005) 155426.
[17] R.G. Farber, M.E. Turano, E.C.N. Oskorep, N.T. Wands, E.V. Iski, D.R. Killelea, The quest for stability: structural dependence of Rh(111) on oxygen coverage at elevated temperature, J. Phys. Chem. C 121 (2017) 10470–10475.
[18] E.V. Iski, M. El-Kouedi, C. Calderon, F. Wang, D.O. Bellisario, T. Ye, E.C.H. Sykes, The extraordinary stability imparted to silver monolayers by chloride, Electrochim. Acta 56 (2011) 1652–1661.
[19] J.A. Phillips, L.K. Harville, H.R. Morgan, L.E. Jackson, G. LeBlanc, E.V. Iski, Electrochemical control of the thermal stability of atomically thin Ag films on Au (111), Surf. Sci. (2018).
[20] K. Bromann, C. Félix, H. Brune, W. Harbich, R. Monot, J. Buttet, K. Kern, Controlled deposition of size-selected silver nanoclusters, Science 274 (1996) 956–958.
[21] K. Morgenstern, G. Rosenfeld, G. Comsa, Decay of two-dimensional Ag Islands on Ag(111), Phys. Rev. Lett. 76 (1996) 2113–2116.
[22] G. Schulze Icking-Konert, M. Giesen, H. Ibach, Decay of Cu adatom Islands on Cu (111), Surf. Sci. 398 (1998) 37–48.
[23] Q. Guo, F. Yin, R.E. Palmer, Beyond the herringbone reconstruction: magic gold fingers, Small 1 (2005) 76–79.
[24] F. Yin, R.E. Palmer, Q. Guo, Faceting of nanoscale fingers on the (111) surface of gold, Surf. Sci. 600 (2006) 1504–1509.
[25] N. Totó, R. Ferrando, Q. Guo, R.L. Johnston, Nanofinger growth on Au(111) arising from kinetic instability, Phys. Rev. B 75 (2007) 195434.
[26] D. Costa, C.-M. Pradier, F. Tielens, L. Savio, Adsorption and self-assembly of bio-organic molecules at model surfaces: a route towards increased complexity, Surf. Sci. Rep. 70 (2015) 449–553.
[27] K.E. Wilson, H.A. Früchtl, F. Grillo, C.J. Baddeley, (S)-Lysine adsorption induces the formation of gold nanofingers on Au{111}, Chem. Commun. 47 (2011) 10365–10367.
[28] Valentina Arima, R.I.R. Blyth, Francesca Matino, Letizia Chiodo, Fabio Della Sala, Julie Thompson, Tom Regier, Roberta Del Sole, Giuseppe Mele, Giuseppe Vasapollo, Roberto Cingolani, R. Rinaldi, Zinc porphyrin-driven assembly of gold nanofingers, Small 4 (2008) 497–506.
[29] F. Chen, A. Zhou, H. Yang, The effects of strain on STM lithography on HS-ssDNA/Au (111) surface, Appl. Surf. Sci. 255 (2009) 6832–6839.
[30] S.M. Barlow, R. Raval, Complex organic molecules at metal surfaces: bonding, organisation and chirality, Surf. Sci. Rep. 50 (2003) 201–341.
[31] S.M. Barlow, R. Raval, Nanoscale insights in the creation and transfer of chirality in amino acid monolayers at defined metal surfaces, Curr. Opin. Colloid Interface Sci.

13 (2008) 65–73.
[32] Q. Chen, N.V. Richardson, Enantiomeric interactions between nucleic acid bases and amino acids on solid surfaces, Nat. Mater. 2 (2003) 324.
[33] S. Fischer, A.C. Papageorgiou, M. Marschall, J. Reichert, K. Diller, F. Klappenberger, F. Allegretti, A. Nefedov, C. Wöll, J.V. Barth, L-Cysteine on Ag(111): a combined STM and X-ray spectroscopy study of anchorage and deprotonation, J. Phys. Chem. C 116 (2012) 20356–20362.
[34] C. Joachim, J.K. Gimzewski, A. Aviram, Electronics using hybrid-molecular and mono-molecular devices, Nature 408 (2000) 541.
[35] L. Romaner, G. Heimel, M. Gruber, J.-L. Brédas, E. Zojer, Stretching and breaking of a molecular junction, Small 2 (2006) 1468–1475.
[36] N.L. Rosi, C.A. Mirkin, Nanostructures in Biodiagnostics, Chem. Rev. 105 (2005) 1547–1562.
[37] V. Kacaniklic, K. Johansson, G. Marko–Varga, L. Gorton, G. Jönsson–Pettersson, E. Csöregi, Amperometric biosensors for detection of L- and D-amino acids based on coimmobilized peroxidase and L- and D-amino acid oxidases in carbon paste electrodes, Electroanalysis 6 (1994) 381–390.
[38] A.M. Bond, P.A. Lay, Cyclic voltammetry at microelectrodes in the absence of added electrolyte using a platinum quasi-reference electrode, J. Electroanal. Chem. Interfacial Electrochem. 199 (1986) 285–295.
[39] M. Azhagurajan, T. Itoh, K. Itaya, Ultra-high-resolution differential interference microscopy of Ag deposition on an ultraflat Au(111), J. Phys. Chem. C 120 (2016) 16221–16227.
[40] K. Itaya, E. Tomita, Scanning tunneling microscope for electrochemistry – a new concept for the in situ scanning tunneling microscope in electrolyte solutions, Surf. Sci. 201 (1988) L507–L512.
[41] K. Ogaki, K. Itaya, In situ scanning tunneling microscopy of underpotential and bulk deposition of silver on gold (111), Electrochim. Acta 40 (1995) 1249–1257.
[42] D.M. Kolb, J. Schneider, Surface reconstruction in electrochemistry: au(100-(5 × 20), Au(111)-(1 × 23) and Au(110)-(1 × 2), Electrochim. Acta 31 (1986) 929–936.
[43] O.M. Magnussen, J. Hotlos, R.J. Nichols, D.M. Kolb, R.J. Behm, Atomic structure of Cu adlayers on Au(100) and Au(111) electrodes observed by in situ scanning tunneling microscopy, Phys. Rev. Lett. 64 (1990) 2929–2932.
[44] D.A. Scherson, D.M. Kolb, Voltammetric curves for Au(111) in acid media: a comparison with Pt(111) surfaces, J. Electroanal. Chem. Interfacial Electrochem. 176 (1984) 353–357.
[45] J. Wiechers, T. Twomey, D.M. Kolb, R.J. Behm, An in-situ scanning tunneling microscopy study of au (111) with atomic scale resolution, J. Electroanal. Chem. Interfacial Electrochem. 248 (1988) 451–460.
[46] X. Gao, A. Hamelin, M.J. Weaver, Atomic relaxation at ordered electrode surfaces probed by scanning tunneling microscopy: au(111) in aqueous solution compared with ultrahigh-vacuum environments, J. Chem. Phys. 95 (1991) 6993–6996.
[47] A. Hamelin, Cyclic voltammetry at gold single-crystal surfaces. Part 1. Behaviour at low-index faces, J. Electroanal. Chem. 407 (1996) 1–11.
[48] A. Hamelin, The crystallographic orientation of gold surfaces at the gold-aqueous solution interphases, J. Electroanal. Chem. Interfacial Electrochem. 142 (1982) 299–316.
[49] T. Dretschkow, A.S. Dakkouri, T. Wandlowski, In-situ scanning tunneling microscopy study of uracil on Au(111) and Au(100), Langmuir 13 (1997) 2843–2856.
[50] H. Angerstein-Kozlowska, B.E. Conway, A. Hamelin, L. Stoicoviciu, Elementary steps of electrochemical oxidation of single-crystal planes of Au Part II. A chemical and structural basis of oxidation of the (111) plane, J. Electroanal. Chem. Interfacial Electrochem. 228 (1987) 429–453.
[51] A.J. Bard, L.R. Faulkner, Electrochemical Methods: Fundamentals and Applications, Wiley, 2000.
[52] J.A. Polta, D.C. Johnson, The direct electrochemical detection of amino acids at a platinum electrode in an alkaline chromatographic effluent, J. Liq. Chromatogr. 6 (1983) 1727–1743.
[53] T.R. Ralph, M.L. Hitchman, J.P. Millington, F.C. Walsh, The electrochemistry of L-cystine and L-cysteine: part 1: thermodynamic and kinetic studies, J. Electroanal. Chem. 375 (1994) 1–15.
[54] F. Huerta, E. Morallón, F. Cases, A. Rodes, J.L. Vázquez, A. Aldaz, Electrochemical behaviour of amino acids on Pt(h,k,l): a voltammetric and in situ FTIR study. Part 1. Glycine on Pt(111), J. Electroanal. Chem. 421 (1997) 179–185.
[55] D. Wang, S.-B. Lei, L.-J. Wan, C. Wang, C.-L. Bai, Effect of chemical structure on the adsorption of amino acids with aliphatic and aromatic substitution groups: in situ STM study, J. Phys. Chem. B 107 (2003) 8474–8478.
[56] H.-Q. Li, A. Chen, S.G. Roscoe, J. Lipkowski, Electrochemical and FTIR studies of L-phenylalanine adsorption at the Au(111) electrode, J. Electroanal. Chem. 500 (2001) 299–310.
[57] A.P. Sandoval, J.M. Orts, A. Rodes, J.M. Feliu, A comparative study of the adsorption and oxidation of L-alanine and L-serine on Au(100), Au(111) and gold thin film electrodes in acid media, Electrochim. Acta 89 (2013) 72–83.
[58] Y.-G. Kim, J.B. Soriaga, G. Vigh, M.P. Soriaga, Atom-resolved EC-STM studies of anion adsorption at well-defined surfaces: Pd(111) in sulfuric acid solution, J. Colloid Interface Sci. 227 (2000) 505–509.
[59] I. Oda, Y. Shingaya, H. Matsumoto, M. Ito, Upd mechanisms of copper and thallium on a Pt(111) electrode studied by in-situ IRAS and EC-STM, J. Electroanal. Chem. 409 (1996) 95–101.
[60] S. Sek, EC-STM study of potential-controlled adsorption of substituted pyrimidinethiol on Au(111), Langmuir 25 (2009) 13488–13492.
[61] Y. Shingaya, H. Matsumoto, H. Ogasawara, M. Ito, In situ and ex situ IRAS, LEED and EC-STM studies of underpotentially deposited copper on a Pt(111) electrode in sulfuric acid solution: coadsorption of sulfate ion with copper, Surf. Sci. 335 (1995) 23–31.
[62] E. Szőcs, I. Bakó, T. Kosztolányi, I. Bertóti, E. Kálmán, EC-STM study of 5-mercapto-1-phenyl-tetrazole adsorption on Cu(1 1 1), Electrochim. Acta 49 (2004) 1371–1378.
[63] C. Vaz-Domínguez, M. Escudero-Escribano, A. Cuesta, F. Prieto-Dapena, C. Cerrillos, M. Rueda, Electrochemical STM study of the adsorption of adenine on Au(111) electrodes, Electrochem. Commun. 35 (2013) 61–64.
[64] P. Kao, S. Neppl, P. Feulner, D.L. Allara, M. Zharnikov, Charge transfer time in alkanethiolate self-assembled monolayers via resonant auger electron spectroscopy, J. Phys. Chem. C 114 (2010) 13766–13773.
[65] M.M. Maitani, T.A. Daniel, O.M. Cabarcos, D.L. Allara, Nascent metal atom condensation in self-assembled monolayer matrices: coverage-driven morphology transitions from buried adlayers to electrically active metal atom nanofilaments to overlayer clusters during aluminum atom deposition on alkanethiolate/gold monolayers, J. Am. Chem. Soc. 131 (2009) 8016–8029.
[66] J.D. Monnell, J.J. Stapleton, S.M. Dirk, W.A. Reinerth, J.M. Tour, D.L. Allara, P.S. Weiss, Relative conductances of alkaneselenolate and alkanethiolate monolayers on Au{111}, J. Phys. Chem. B 109 (2005) 20343–20349.
[67] D.L. Allara, T.D. Dunbar, P.S. Weiss, L.A. Bumm, M.T. Cygan, J.M. Tour, W.A. Reinerth, Y. Yao, M. Kozaki, L. Jones II, Evolution of strategies for self-assembly and hookup of molecule-based devices, Ann. N.Y. Acad. Sci. 852 (1998) 349–370.
[68] S. Frey, A. Shaporenko, M. Zharnikov, P. Harder, D.L. Allara, Self-assembled monolayers of nitrile-functionalized alkanethiols on gold and silver substrates, J. Phys. Chem. B 107 (2003) 7716–7725.
[69] G. Travaglini, H. Rohrer, M. Amrein, H. Gross, Scanning tunneling microscopy on biological matter, Surf. Sci. 181 (1987) 380–390.
[70] A.M. Baró, R. Miranda, J. Alamán, N. García, G. Binnig, H. Rohrer, C. Gerber, J.L. Carrascosa, Determination of surface topography of biological specimens at high resolution by scanning tunnelling microscopy, Nature 315 (1985) 253–254.
[71] R. Guckenberger, C. Kösslinger, R. Gatz, H. Breu, N. Levai, W. Baumeister, A scanning tunneling microscope (STM) for biological applications: design and performance, Ultramicroscopy 25 (1988) 111–121.
[72] N. Knorr, H. Brune, M. Epple, A. Hirstein, M.A. Schneider, K. Kern, Long-range adsorbate interactions mediated by a two-dimensional electron gas, Phys. Rev. B 65 (2002) 115420.
[73] J. Repp, F. Moresco, G. Meyer, K.-H. Rieder, P. Hyldgaard, M. Persson, Substrate mediated long-range oscillatory interaction between adatoms: Cu/Cu(111), Phys. Rev. Lett. 85 (2000) 2981–2984.
[74] E. Wahlström, I. Ekvall, H. Olin, L. Walldén, Long-range interaction between adatoms at the Cu(111) surface imaged by scanning tunnelling microscopy, Appl. Phys. A 66 (1998) 1107–1110.
[75] X. Zhao, H. Wang, R.G. Zhao, W.S. Yang, Self-assembly of amino acids on the Cu (001) surface, Mater. Sci. Eng. C 16 (2001) 41–50.
[76] M. Forster, M.S. Dyer, M. Persson, R. Raval, 2D random organization of racemic amino acid monolayers driven by nanoscale adsorption footprints: proline on Cu (110), Angew. Chem. 122 (2010) 2394–2398.
[77] N.P. Guisinger, A.J. Mannix, R.B. Rankin, B. Kiraly, J.A. Phillips, S.B. Darling, B.L. Fisher, M.C. Hersam, E.V. Iski, Amino acid immobilization of copper surface diffusion on Cu(111), Adv. Mater. Interfaces (2019) 6, 1900021.